Available online at www.sciencedirect.com

ScienceDirect

www.elsevier.com/locate/jes

JES JOURNAL OF ENVIRONMENTAL SCIENCES

www.jesc.ac.cn

Research article

Electrochemically assisted production of biogenic palladium nanoparticles for the catalytic removal of micropollutants in wastewater treatment plants effluent☆

Cindy Ka Y Law[1,2], *Kankana Kundu*[1,2], *Luiza Bonin*[1,2], *Lorena Peñacoba-Antona*[3,4], *Eduardo Bolea-Fernandez*[5], *Frank Vanhaecke*[5], *Korneel Rabaey*[1,2], *Abraham Esteve-Núñez*[3,4,6], *Bart De Gusseme*[1,2], *Nico Boon*[1,2,*]

[1] *Center for Microbial Ecology and Technology (CMET), Ghent University, Coupure Links 653, B-9000 Gent, Belgium*
[2] *Centre for Advanced Process Technology for Urban Resource recovery (CAPTURE), P.O. Frieda Saeysstraat 1, B-9000 Gent, Belgium*
[3] *METfilter S.L., Autovía A49 Sevilla-Huelva Km 28, 41820 Carrión de los Céspedes, Sevilla, Spain*
[4] *IMDEA Water Institute, Av. Punto Com, 2, Parque Científico Tecnológico, 28805 Alcalá de Henares, Madrid, Spain*
[5] *Atomic & Mass Spectrometry (A&MS) research group, Department of Chemistry, Ghent University, Campus Sterre, Krijgslaan 281-S12, B-9000 Ghent, Belgium*
[6] *Universidad de Alcalá, Department of Analytical Chemistry, Physical Chemistry and Chemical Engineering, Ctra. Madrid-Barcelona Km 33.600, 28871 Alcalá de Henares, Madrid, Spain*

ARTICLE INFO

Article history:
Received 30 June 2022
Revised 11 August 2022
Accepted 11 August 2022
Available online 27 August 2022

Keywords:
Antibiotics
Adsorption
Biogenic palladium nanoparticles
Catalytic activity
H_2
Secondary treated municipal wastewater

ABSTRACT

Biogenic palladium nanoparticles (bio-Pd NPs) are used for the reductive transformation and/or dehalogenation of persistent micropollutants. In this work, H_2 (electron donor) was produced *in situ* by an electrochemical cell, permitting steered production of differently sized bio-Pd NPs. The catalytic activity was first assessed by the degradation of methyl orange. The NPs showing the highest catalytic activity were selected for the removal of micropollutants from secondary treated municipal wastewater. The synthesis at different H_2 flow rates (0.310 L/hr or 0.646 L/hr) influenced the bio-Pd NPs size. The NPs produced over 6 hr at a low H_2 flow rate had a larger size (D50 = 39.0 nm) than those produced in 3 hr at a high H_2 flow rate (D50 = 23.2 nm). Removal of 92.1% and 44.3% of methyl orange was obtained after 30 min for the NPs with sizes of 39.0 nm and 23.2 nm, respectively. Bio-Pd NPs of 39.0 nm were used to treat micropollutants present in secondary treated municipal wastewater at concentrations ranging from μg/L to ng/L. Effective removal of 8 compounds was observed: ibuprofen (69.5%) < sulfamethoxazole (80.6%) < naproxen (81.4%) < furosemide (89.7%) < citalopram (91.7%) < diclofenac (91.9%) < atorvastatin (> 94.3%) < lorazepam (97.2%). Re-

☆ https://www.cmet.ugent.be/.

* Corresponding author.
E-mail: Nico.Boon@UGent.be (N. Boon).

https://doi.org/10.1016/j.jes.2022.08.018

moval of fluorinated antibiotics occurred at > 90% efficiency. Overall, these data indicate that the size, and thus the catalytic activity of the NPs can be steered and that the removal of challenging micropollutants at environmentally relevant concentrations can be achieved through the use of bio-Pd NPs.

Introduction

Anthropogenic activities are rapidly exacerbating environmental pollution (Gautam et al., 2019). Pharmaceuticals and various chemical compounds of environmental concern are present in many products used daily. These products are a significant source of pollution, reaching a broadening area through the effect of greater urbanization worldwide. Although effective removal of macropollutants is achieved through traditional wastewater treatment plants (WWTP), this is not the case for micropollutants. Micropollutants such as antibiotics, personal care products, detergents, and dyes, are rarely controlled before the discharge of the wastewater into the environment, as their removal at low concentrations lacks effectiveness (de Andrade et al., 2018; Jiang et al., 2020; Pandey et al., 2020). The presence of micropollutants in the environment is undesirable due to their impact on the ecosystem and human health (Pandey et al., 2020). One of the emerging micropollutants is antibiotics, which are mainly used to cure diseases in humans and animals (Cao et al., 2017). The presence of this in the environment has severe adverse consequences on their effectiveness for curing diseases due to the development of (multi-) resistant bacteria and genes (Cao et al., 2017; Liu et al., 2019; Jiang et al., 2020). Dyes are also used broadly in the industry for, *e.g.*, cosmetics, pharmaceuticals, paper, and agricultural compounds (Khataee and Kasiri, 2010). They have been associated with mutagenic and carcinogenic repercussions for human health (Pandey et al., 2020). Therefore, it is important to remove these micropollutants effectively and avoid their discharge into the environment.

Common techniques for the removal of antibiotics and dyes are adsorption, membrane filtration, and advanced oxidation processes (AOP) (Abtahi et al., 2018; de Andrade et al., 2018; Pandey et al., 2020). Adsorption and membrane filtration are only temporary solutions in which, the micropollutants are transferred away from the wastewater rather than being treated (degradation in metabolites), while the wastestream also contains a high ionic load (cations and anions) (Bobu et al., 2013; Yagub et al., 2014). The disadvantages of AOP are the high energy consumption and costs, as well as the production of secondary toxic wastestreams (Abtahi et al., 2018; Anjali and Shanthakumar, 2019). Therefore, it is essential to find an environmentally friendly and highly efficient method that does not produce toxic and high concentrated wastestreams alongside the removal of antibiotics and dyes. The use of biogenic palladium nanoparticles (bio-Pd NPs) for the removal of pharmaceutical compounds and dyes has been tested with promising results (Forrez et al., 2011; Wang et al., 2018). However, the application of bio-Pd NPs for the removal of fluorinated pharmaceutical compounds (*e.g.*, ciprofloxacin, citalopram, and atorvastatin), which are highly used and for which removal efficiencies tend to be low, have not been well studied yet (Forrez et al., 2011; Miao et al., 2018; Osawa et al., 2019; Antonelli et al., 2020). Martins et al. (2017), assessed the removal of several antibiotics by bio-Pd NPs, but no removal of fluorinated antibiotics as a result of the catalytic activity of the NPs was detected. The study was carried out in a synthetic medium, where the matrix composition is fairly simple in contrast to real environmental matrices. Nevertheless, a removal of 87.7% of ciprofloxacin was found after 25 hr and at pH = 3.2 with 30 mg of Pd in the form of bio-Pd NPs (He et al., 2020). The disadvantage of this method is the low pH and high concentrations of Pd needed. Moreover, the degradation of persistent fluorinated antibiotics, other than ciprofloxacin, with bio-Pd NPs required further study, especially in environmentally relevant matrices. Ideally, effective removal is accomplished with the use of a lower concentration of Pd, shorter reaction time, higher pH, and in environmentally relevant concentrations are required.

Bio-Pd NPs have been thoroughly studied for the removal of various chlorinated compounds (De Corte et al., 2012; De Gusseme et al., 2012; Hazarika et al., 2017; He et al., 2020). Synthesis is often accomplished by the microorganisms *Shewanella oneidensis* due to its metal-reducing properties (Lovley, 1993; Dundas et al., 2018). The formation of bio-Pd NPs also requires the addition of an electron donor such as H_2, which is the most suitable electron donor for *S. oneidensis*, due to their intrinsic metabolism (Yang et al., 2020). Three mechanisms occur in the formation of bio-Pd NPs, (1) biological conversion from Pd^{2+} to Pd^0 by microorganisms, (2) chemical conversion of palladium with H_2, and (3) autocatalytic conversion of palladium (Yang et al., 2020). The latter two processes result in the formation of large nanoparticle clusters due to the aggregation of the NPs (Deplanche et al., 2014). Large NPs is not desired because of its low surface/volume ratio, whereas the catalytic activity depends on the size of the bio-Pd NPs (Saldan et al., 2015). Current research targets the production of smaller bio-Pd NPs. De Windt et al. (2006) and Hou et al. (2017) studied the influence of cell viability by employing different Pd:Cell Dry Weight (CDW) ratios. Nevertheless, Pd:CDW ratios alongside other production parameters can be tested over virtually unlimited ranges. The production of bimetallic bio-Pd NPs has also been extensively studied, with the second metal often being catalytically active as well (Tuo et al., 2017; Gomez-Bolivar et al., 2019; Omajali et al., 2019; Sivamaruthi et al., 2019). In this way, the catalytic activ-

ity of the bio-Pd NPs can be increased by the second metal, resulting in a higher removal efficiency of the micropollutants (Omajali et al., 2019). The disadvantage of this method is that the addition of a second metal increased the costs and that additional steps are needed before and after production. It is also possible to enhance the catalytic activity by reshaping the microorganisms and attached palladium nanoparticles through the use of an activation agent such as potassium hydroxide (KOH) (Xiong et al., 2018). Although the catalytic activity increases, the conditions to obtain the change in morphology are stringent and expensive to maintain. Therefore, finding a more feasible method to control or steer the production of the bio-Pd NPs size is a high priority.

In this work, the production of different sized bio-Pd NPs was controlled by: (1) adsorption of Pd^{2+} on *Shewanella oneidensis* (biosorption) before the exposure to the electron donor H_2 (0 hr, 24 hr, and 48 hr), (2) low (0.310 L/hr) and high (0.646 L/hr) H_2 concentrations in the liquid phase, and (3) the contact time (3 hr or 6 hr) between H_2, Pd^{2+}, and *Shewanella oneidensis*. H_2 was produced by an electrochemical cell (EC) to control the availability of H_2, and thus, to steer the size of bio-Pd NPs. When bio-Pd NPs are produced, an electron donor is required to reduce Pd^{2+} to Pd^0 microbially (Yang et al., 2020), therefore, the concentration of electron donor was never controlled by an electrochemical system before. Here, H_2, electrochemically produced, will be used by the microbial cells to convert the palladium, but will also be used for chemical and autocatalytic conversion of Pd^{2+} to Pd^0. The catalytic activity of the different bio-Pd NPs was first tested using methyl orange. Based on the results obtained for the removal of methyl orange, the bio-Pd NPs with the highest removal efficiency was selected and used for the removal of a mixture of micropollutants (including fluorinated antibiotics) present in the secondary treated municipal wastewater. Here, 25 different compounds were detected, of which 8 compounds are discussed in detail.

1. Materials and methods

1.1. Chemicals

The Na_2PdCl_4 powder (98%), phosphate-buffered saline (PBS) tablets, Luria Bertani (LB) used for bio-Pd NPs production, and methyl orange for the activity test were purchased from Merck (Merck, Germany). The M9 medium used for washing the bio-Pd NPs was prepared based on the recipe provided by Merck and contained KH_2PO_4, Na_2HPO_4, NaCl and NH_4Cl purchased from Carl Roth (Carl Roth, Germany). The KOH tablets used as electrolyte was purchased from Carl Roth. For ICP-MS analysis, ultra-pure water (resistivity > 18.2 MΩ cm, Millipore, France) was used. Pro analysis purity level 14 mol/L HNO_3 (ChemLab, Belgium), further purified by sub-boiling distillation, and 9.8 mol/L H_2O_2 (Fluka, Belgium) were used for acid digestion. 1 g/L single-element standard solutions of Pd and Rh (Instrument Solutions, The Netherlands) were used for method development and calibration purposes, and for internal standardization, respectively.

1.2. Bio-Pd NPs solution preparation

The production of bio-Pd NPs was carried out as described by De Windt et al. (2005). *Shewanella oneidensis* MR-1 cells were grown in LB medium overnight at 28°C on a shaker (New Brunswick Scientific, Belgium) and harvested by centrifuging at 10,000 ×g for 10 min. The cells were washed three times with M9 medium and resuspended in M9 medium to a final optical of $OD_{610} = 0.5$ with Spectronic 200 (Thermofischer, USA). The Na_2PdCl_4 was added to the resuspended solution at a concentration of 50 mg/L Pd^{2+}; this solution was incubated overnight on a shaker at 20°C (Appendix A **Table S1**.). Production of different types of bio-Pd NPs (Appendix A **Table S1.**) was performed in a custom-built experimental setup (Fig. 1). Corresponding controls were prepared in the same manner

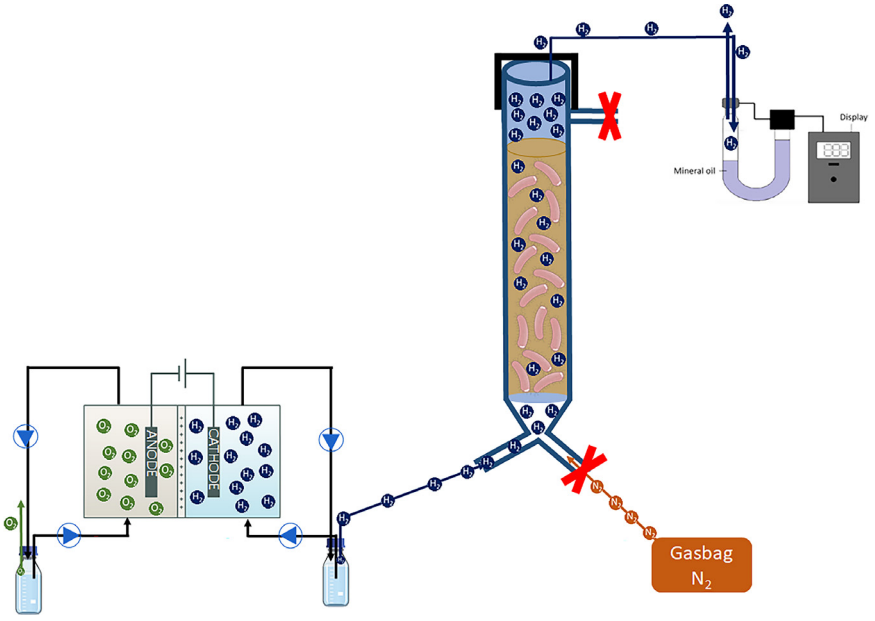

Fig. 1 – Experimental setup for a steered bio-Pd NPs production through the use of an EC.

but were not exposed to H_2. The bio-Pd NPs produced and controls were washed three times with PBS and stored at 5°C.

1.3. Experimental setup for bio-Pd NPs production

A custom-built experimental setup (in triplicate) containing an EC connected to a glass column was used to produce bio-Pd NPs. A two-compartment EC (dimensions: 23.5 × 9.0 × 2.5 cm) made from two Perspex® frames was used to separate the cation exchange membrane (CEM) (Membrane International Inc., USA) from the electrodes. A stainless-steel electrode was used as the cathode (dimensions: 5 × 20 cm) and an iridium electrode was used as the anode. Between the compartments and CEM, rubber sheets were placed to create a liquid-tight seal, and the frames were bolstered. A pump at a flow rate of 252 mL/min (Watson Marlow NV, Belgium), was used to recirculate the KOH electrolyte. The current of the EC was controlled by a power supply (Velleman, Belgium), Faraday's Law was used to calculate the amount of H_2 produced based on the current applied. The EC was connected to a glass column (wrapped in aluminum foil to prevent light penetration), in which the microorganisms/Pd^{2+} solution was transferred in, after incubation. The top of the glass column was connected to a gascounter. The bottom of the column contained a two-way connector between the EC and a gasbag for N_2 flushing, both regulated by a valve.

1.4. Bulk ICP-MS analysis and TEM images

Bulk ICP-MS, Agilent 8800 ICP-MS instrument (Agilent Technologies, Japan), analysis was performed to determine the concentration of Pd in the different bio-Pd NP samples. The TEM JEOL JEM 1010 (Jeol, Japan) images were taken to confirm the particle size. The D50 particle size was determined by ImageJ software.

For bulk analysis, the bio-Pd samples were acid digested in closed Savillex® PFA beakers prior to ICP-MS. 5 mL of suspended bio-Pd in PBS was centrifuged at 10,000 ×g for 30 min, after which the supernatant was removed. The resulting pellet was acid digested with 1.5 mL of 14 mol/L HNO_3 and 0.5 mL of 9.8 mol/L H_2O_2. The closed beakers were heated to 115°C overnight on a hot plate. After complete mineralization, the digestates were evaporated at 90°C until dryness, then redissolved in 2.0 mL of 0.35 mol/L HNO_3. This solution was further diluted with 0.35 mol/L HNO_3 and Rh was added as the internal standard (final concentration = 2 µg/L) to compensate for potential matrix effects and/or signal instability.

For TEM analysis, 1.0 mL suspended bio-Pd in PBS was centrifuged at 5000 ×g for 5 min and washed three times with 1.0 mL ultra-pure water (Millipore, France). Subsequently resuspended in 1.0 mL of ultra-pure water. 2.0 µL of the solution was placed on the formvar-coated Cu single slot grid (Agar, UK), dried for 20 min at 37°C spent overnight in the Jeol EM-DSC20 vacuum chamber (Jeol, Japan). The TEM images were taken with a Jeol JEM 1010 TEM at 60 kV, equipped with a side-mounted charge coupled device (CCD) Veleta camera (EMSIS GmbH, Germany).

1.5. Catalytic activity test with methyl orange

The catalytic activity of bio-Pd NPs was evaluated by the removal of 100 mg/L Methyl Orange (in biological triplicates), in serum flasks. Suspended bio-Pd was centrifuged at 10,000 ×g for 10 min, and the pellet of centrifuged bio-Pd corresponded to 80.95 µg Pd. The pellet was resuspended in 19.2 mL of distilled water and 0.8 mL of Methyl Orange stock solution (7.63 mmol/L) was added. The serum flasks were flushed with 100% N_2 for 20 cycles, subsequently, 120 mL of 100% H_2 was added. 1 mL sample was taken at 0, 10, 15, 30, 50, 70, 90, 110, and 120 min and was filtered using a 0.20 µm filter. The absorbance was measured at a λ_{max} = 465 nm using a Spectronic 200 (ThermoFischer, USA). Distilled water and (filtered) suspended bio-Pd in distilled water were used as a control for the absorbance measurements. Suspended microorganisms without Pd were used as a control for the catalytic activity test.

1.6. Removal of emerging compounds from secondary treated municipal wastewater

Removal of micropollutants in secondary treated wastewater (in duplicate) was tested with the bio-Pd NPs showing the highest activity, as selected based on the results of Section 1.5. The raw wastewater first went through primary treatment, whereafter the effluent went to secondary treatment, described elsewhere (Peñacoba-Antona et al., 2021). A sample of this secondary treated wastewater was taken, representing t_0 = 0 min. The removal of the micropollutants present in the secondary effluent was performed with centrifuged 9.41 mg Pd, resuspended the pellet in 700 mL of secondary effluent in 1 L Schott bottles. The Schott bottles were wrapped in aluminum foil and flushed with 100% N_2 for 20 cycles, whereafter 240 mL of H_2 (100%) was immediately added and another 240 mL of H_2 (100%) was added 1 hr later and was placed on a stirrer. Samples were taken at 2 hr and 24 hr and were centrifuged at 10,000 ×g for 10 min. The supernatants were filtered through a 0.20 µm filter. Secondary effluent with only H_2 and autoclaved *Shewanella oneidensis* with H_2 were used as controls for the test.

1.7. Detection of the emerging compounds

The micropollutants were extracted with a multi-residue method (solid-phase extraction) from the treated secondary effluent and were detected with LC-MS/MS, described in detail elsewhere (de Santiago-Martín et al., 2020). An aliquot (100 mL) of the sample was passed through an Oasis HLB cartridge (200 mg, 6 cc, Waters, USA) and eluted with methanol. Two chromatographic separations were necessary. In positive ionization mode, the Kinetex Biphenyl column (50 × 3 mm, 2.7 µm, Phenomenex, Torrance, CA, USA) was used. The mobile phases were 0.1% (V/V) formic acid in ultrapure water (phase A) and 0.1% (V/V) formic acid in MeOH (phase B). Compounds in negative ionization mode were separated using the Poroshell 120 EC-C18 column (50 × 3 mm, 2.7 µm, Agilent Technologies). The mobile phases used were 5 mmol/L ammonium fluoride in ultrapure water (phase A) and MeOH:MeCN (65.35, V/V) (phase B). For both separations, the flow rate of the mobile phase was 0.6 mL/min, and the sample injection volume of 20 µL.

2. Results and discussion

2.1. *Small nanoparticles are formed with high continuous availability of H_2*

The influence of (1) the adsorption (biosorption) of Pd^{2+} on *Shewanella oneidensis*, (2) the contact time between H_2, Pd^{2+}, and the microorganisms, as well as (3) the flow rate of H_2 (thus the availability of H_2 in the liquid phase) on the production of bio-Pd NPs was studied (Appendix A **Table S1.**). Large nanoparticles (D50 = 140.0 nm, condition 1) were obtained when no adsorption of Pd^{2+} on the microorganisms took place, while smaller nanoparticles (< 100 nm) were obtained for all conditions with adsorption before the exposure to H_2. When comparing the controls of incubated and non-incubated cells, it was observed that adsorption was present for the incubated cells and that NPs were present in cells that were exposed to H_2. Adsorption on the cell surface was observed by TEM images, when comparing incubated and non-incubated cells, furthermore, this has also been found by other researchers (Xu et al., 2018). The ICP-MS data of the controls (Appendix A **Fig. S1**.) also showed a difference in Pd conversion efficiency between the cells incubated for 24 hr and 48 hr. Together, with the TEM images, it can be confirmed that adsorption was present. The ICP-MS data of the controls showed that there was a maximum Pd conversion efficiency of 11.7%, while in the presence of H_2 the conversion of Pd was minimal 26.9%. Hence it can be stated that H_2 is required for the synthesis of bio-Pd NPs, as this is responsible for the majority of Pd conversion, but *Shewanella oneidensis* is also able to convert Pd alone as shown before in the literature (Yang et al., 2020). Nevertheless, adsorption has a strong influence on the particle size. In this work, it was hypothesized that smaller NPs would be produced when the adsorption time was longer as this causes higher adsorption of Pd^{2+} and subsequently higher biological conversion. However, the opposite behavior was observed here – larger nanoparticles were produced with a longer adsorption time (condition 6). The long adsorption time (48 hr) possibly inactivated the microorganisms, a hypothesis supported by the observations made by He et al. (2020), and Chen and Chen (2021). Maximal adsorption was reported by *E. coli* after 2 hr when all the sorption sites on the microorganisms were occupied by Pd^{2+} causing saturation (He et al., 2020). When high concentrations of Pd^{2+} are present in the microorganisms, this destroys the activity of the reactive oxygen scavenging enzymes. This results in high amounts of reactive oxygen species (ROS), causing bacterial damage and ultimately death, as found for *Bacillus wiedmannii* (Chen and Chen, 2021). Production of small bio-Pd NPs in the biosorption process was also observed here, which corresponds to the findings from the literature (Xu et al., 2018). The produced bio-Pd NPs can autocatalytically convert the attached Pd^{2+} on the already formed bio-Pd NPs, with the longer reaction time contributing to the higher autocatalytic conversion and resulting in larger NPs.

When comparing condition 2 (23.2 nm) and 3 (53.2 nm) in which, bio-Pd NPs are produced at a high flow rate of H_2 (0.646 L/hr H_2), it was observed that larger NPs were obtained when the contact time between H_2, Pd^{2+}, and the microorganisms was longer (6 hr). In contrast, smaller NPs, condition 5 (39.0 nm) compared to 4 (75.6 nm), were obtained when a lower flow rate (0.310 L/hr H_2) and a longer exposure time with H_2 (6 hr) were used. Hence, contradictory data were obtained for the two exposure times and H_2 flow rates. This is because the exposure time depends on the H_2 flow rate, thus the availability of H_2 in the liquid phase, which is confirmed when comparing condition 2 with 5, and 3 with 4. The availability of H_2 produced during 6 hr with 0.310 L/hr is equal to that produced during 3 hr with 0.646 L/hr. The use of a longer exposure time and a higher H_2 flow rate results in a higher degree of chemical and autocatalytic conversion, and hence, agglomeration as a result of which larger nanoparticles are produced. Nevertheless, a long exposure time is required with a low H_2 flow rate to have sufficient H_2 for the biological conversion of Pd^{2+}. Different conversions from Pd^{2+} to Pd^0 were found when different formate concentrations were tested, with the highest reductions (99%) of Pd^{2+} when a 25-fold higher formate concentration was used compared to the lowest formate concentration used in that study (Yang et al., 2020). However, different observations were found in this work. The greater solubility of formate over H_2 leads to its preferential uptake in solution. Therefore, the *in situ* production of H_2 is necessary to steer the size of the nanoparticles during bio-Pd NPs synthesis.

2.2. *The size of the nanoparticles is independent of the conversion efficiency of Pd^{2+} to Pd^0*

The conversion efficiency of Pd^{2+} into bio-Pd NPs was determined through ICP-MS, which allowed the determination of the average mass of Pd in and around the cells (**Fig. 2A**). High conversion efficiencies were observed for condition 1 (50.1% ± 6.8%) and 6 (44.8% ± 7.4%), which corresponds to a D50 nanoparticle size of 140.0 nm and 62.8 nm respectively. Strong chemical and autocatalytic conversion were present for condition 1 and 6, which was confirmed by the TEM images (**Fig. 2B**). The size of the latter conditions was 2-fold larger, while the difference in conversion efficiency between condition 1 and 6 was only 5.3%. The differences in size and conversion efficiency between the two conditions do not vary in a linear way, which is due to the prior adsorption of Pd^{2+} for 48 hr. The adsorption of Pd^{2+} on the microorganisms is responsible for 11.7% (Appendix A **Fig. S1**) of the conversion efficiency. When this adsorption is not taken into consideration, then only 33.1% of the conversion efficiency originated from the nanoparticles formed, which is similar for condition 2, 3, 4, and 5. Hence, this confirms that the adsorption time of 48 hr caused the production of large NPs (see Section 2.1).

Similar conversion efficiencies could be seen for condition 2, 3, 4 and 5, *i.e.* 31.8% ± 1.4 %, 33.8% ± 2.0 %, 30.2% ± 5.3% and 26.9% ± 5.2% respectively. This corresponded to a D50 particle size of 23.2 nm, 53.2 nm, 75.6 nm, and 39.0 nm respectively. While the variation in size is large, the difference in conversion efficiency is low based on the controls the influence of the adsorption of Pd^{2+} on *Shewanella oneidensis* before the exposure of H_2 can be considered negligible (Appendix A **Fig. S1**). This can be explained by the number of nanoparticles present around the cells, when condition 2 and 5 are compared, the difference in size is 3-fold while this is not the case for the conversion efficiency. The difference is not caused by the adsorption, as for both conditions, the amount of Pd^{2+} ad-

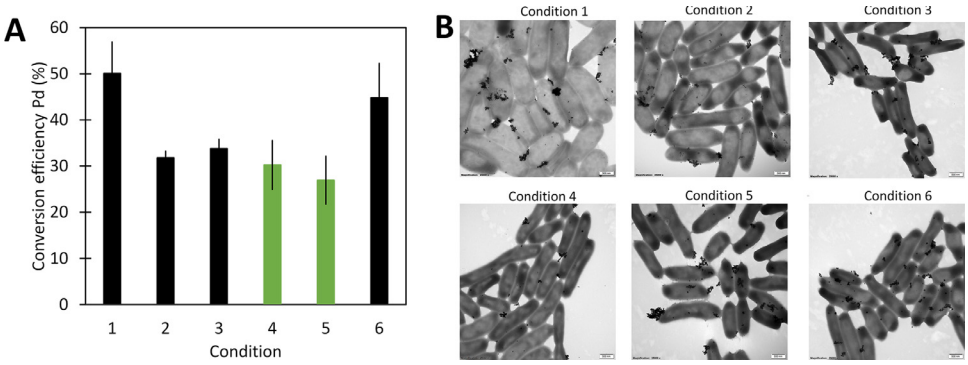

Fig. 2 – A: The conversion efficiency of Pd into bio-Pd NPs as determined by ICP-MS. The different conditions are indicated on the X-axis and the conversion efficiency of Pd on the Y-axis. B: The corresponding TEM images of the different types of bio-Pd NPs.

sorbed is similar. Consequently, the difference is likely caused by the distribution and hence the number of nanoparticles around the cells. When small nanoparticles are formed, it was observed that a high number of nanoparticles are present. The absence of agglomeration indicates that mainly biological conversion is present. The high number of small nanoparticles under condition 2 compared to 4 can be seen in the TEM images (Fig. 2B). Furthermore, it can be concluded that the increase in the size of nanoparticles corresponds with a decrease in the number of nanoparticles. This statement was concise with the finding of De Windt et al. (2006), where it was observed that a low number of nanoparticles were found when the nanoparticle size was large.

2.3. *The highest catalytic activity for the removal of methyl orange was not obtained with the smallest NPs*

The catalytic activity of the different bio-Pd NPs (80.95 µg Pd was used) was tested through the degradation of 100 mg/L methyl orange (Fig. 3), by measuring the decolorization at $\lambda_{max} = 465$ nm. Once methyl orange is decolorized, it was assumed that this compound was degraded into intermediates. It was proposed by Nguyen et al., 2018, in which Pd doped TiO_2 was used for photocatalysis, such that the N – C and azo bonds (-N=N-) were specifically targeted (Nguyen et al., 2018).

High removal of methyl orange was demonstrated for all different types of bio-Pd NPs, except for condition 1. This is due to the large size of the nanoparticles, resulting in a low surface/volume ratio, and hence low catalytic activity (De Windt et al., 2006). Complete degradation was found after 120 min for condition 3, 4, and 5, with condition 5 showing the highest removal efficiency, the D50 nanoparticles' sizes were 53.2 nm, 75.6 nm, and 39.0 nm respectively. The removal efficiencies found for these three conditions were: 99.0% ± 0.8%, 99.5% ± 0.4%, and 99.7% ± 0.2% respectively. It was expected that condition 2 with the smallest nanoparticles would contribute to the highest catalytic activity of the bio-Pd NPs (De Windt et al., 2006; Rotaru et al., 2012; Saldan et al., 2015). However, the catalytic activities from high to low for the different conditions were 5 > 4 > 3 > 6 > 2, which corresponds to NPs sizes of 39.0 nm > 75.6 nm > 53.2 nm > 62.8 nm > 23.2 nm, respectively. While the difference in size is not large,

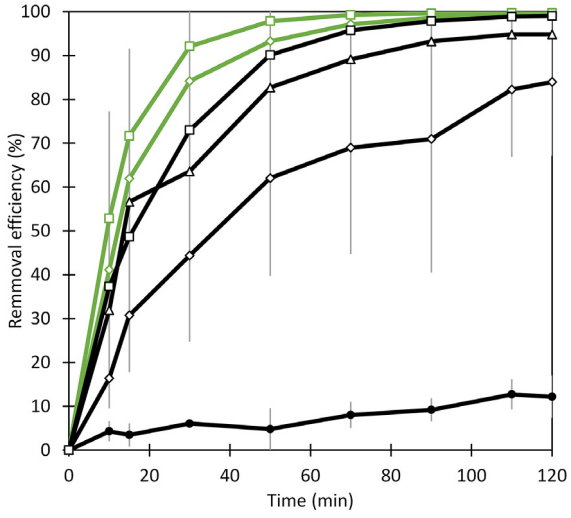

Fig. 3 – The catalytic activity of the different bio-Pd NPs (80.95 µg Pd) as tested using 100 mg/L of methyl orange. The time is plotted on the X-axis and the removal efficiency for methyl orange on the Y-axis. Removal efficiency of the different bio-Pd NPs, condition 1 (●), condition 2 (◇), condition 3 (□), condition 4 (◇), condition 5 (△) and condition 6 (▽).

between condition 2 and 5, the difference in activity rather is. The high activity of condition 5, where 99.7% ± 0.2% removal efficiency was established within 120 min can be explained by the small size of the Pd NPs spread over the microorganism, which is following the findings by De Windt et al. (2006). The low removal of the bio-Pd NPs of condition 2 (84.0% ± 16.7% in 120 min), was not expected. However, besides the size, the catalytic activity of the NPs is also affected by defects, and modifications of the metal by light elements, *e.g.* oxidation, and dissolution of hydrogen and/or carbon (Yudanov et al., 2011). It is possible that the higher number of small NPs present on the cells in condition 2, caused the disintegration of the microbial cells, resulting in the release of carbon, and thereby influencing the catalytic activity. Furthermore, it was found by Yudanov et al. (2011), that structures of

truncated octahedron, which exhibits bulk-like face-centered cubic are the most stable, while non-crystallographic packings, like icosahedron- or decahedron-based shapes shows competition in between small clusters of metal clusters. The density function showed that icosahedral structures are energetically preferred over the face cubic center-based cuboctahedral structures (Yudanov et al., 2011). However, within the octahedron structure, different metal clusters are present, resulting in different adsorption positions, found for CO bindings (Yudanov et al., 2003). Therefore, it is possible that condition 2 had less favorable clustering of the metal particles, causing a lower catalytic activity. Condition 3 had higher activity than 6 due to the smaller size of NPs. However, the high activity of condition 4 was not anticipated, hence all the bio-Pd NPs produced at a lower H_2 flow rate showed better catalytic activity. It was found that the activity is independent of the NPs for a size range between, 2.5 – 6.6 nm (Ershov et al., 2014). However, this is not the case here, as the size difference in the NPs is larger. The following hypothesis is made for the high catalytic activity of bio-Pd NPs formed under condition 4. During the 3 hr production of bio-Pd NPs, the formed nanoparticles possibly adsorbed the H_2 present in the solution for bio-Pd NPs production. Due to the large size of NPs, a large number of H_2 molecules could be adsorbed on the surface. Therefore, it is feasible that the catalytic activity and the high concentration of the adsorbed H_2 on the nanoparticles resulted in a higher removal of the methyl orange than with the smaller nanoparticles formed under condition 3, 6, and 2. Furthermore, it is also possible that condition 4 had a high number of NPs distributed on the microorganisms. However, the effect of the large (condition 4) and small (condition 2) nanoparticle size for the high and low removal needs to be further investigated. Nevertheless, compared to the literature, condition 2, 3, 4, 5, and 6 had a higher removal efficiency for methyl orange (Freitas et al., 2021). Freitas et al. (2021) produced chemical Pd NPs with maghemite as support for the NPs. Although small NPs sizes were obtained, 5 nm, decolorization of only 79% in 240 min was achieved, which needed 2-fold more time and had lower removal efficiency than condition 2 (Freitas et al., 2021).

2.4. *Removal of micropollutants in secondary treated wastewater is observed by bio-Pd NPs*

The bio-Pd NPs with the highest catalytic activity (Section 2.3) were selected and tested for the removal of a diverse mixture of micropollutants present in the secondary treated effluent, also referred as WWTP effluent in this paper. Wastewater (ww) coming from a treatment plant was used because of the environmentally relevant matrix and realistic concentrations of the micropollutants (ng/L – µg/L). In this complex matrix, 25 compounds were selected to determine the removal efficiency (Appendix A **Table S2**). However, the main focus will be on 8 compounds, atorvastatin, citalopram, diclofenac, furosemide, ibuprofen, lorazepam, naproxen, and sulfamethoxazole (**Table 1**). These compounds were chosen due to their frequent use and the poor investigation that has been performed on these micropollutants.

Although low amounts of Pd (13.4 mg/L Pd wastewater) were used, high removal efficiencies for all compounds were obtained after 2 hr treatment, > 69%. From low to high, the removal efficiency was as follows: ibuprofen < sulfamethoxazole < naproxen < furosemide < citalopram < diclofenac < atorvastatin < lorazepam. The additional removal of the pollutants after 24 hr treatment was considered to be irrelevant. The removal rate after 24 hr was low compared to the removal rate established after 2 hr, this might be due to the binding sites of the Pd-H NPs (Han et al., 2009). When high numbers of micropollutants are present, all the Pd-H NPs sites are occupied for the degradation of these pollutants. As degradation of the micropollutants proceeds, intermediates are formed, therefore it was hypothesized that a further degradation of these intermediates is possible. Consequently, with the increase in compounds to be degraded, the occupation of the Pd-H NPs is low versus the high number of pollutants, hence low removal of compounds was obtained after 24 hr.

Removal of the micropollutants is obtained through the catalytic activity of the bio-Pd NPs, which can be confirmed by the controls (Appendix A **Table S2**). It can be seen that neither the microorganisms present in the secondary effluent nor the inactive *Shewanella oneidensis* were able to remove the compounds by adsorption or biodegradation. Furosemide, citalopram, diclofenac, atorvastatin, and lorazepam are halogenated compounds, which showed a removal of > 90%. Bio-Pd NPs are widely used for carbon-carbon and carbon-heteroatom cross-coupling reactions, hydrogenation, and dehalogenation reactions (Hennebel et al., 2011; Adams et al., 2014). Despite that, it can be seen that the dehalogenation reaction is preferred over the other reactions (**Table 1**). It is hypothesized that the removal of furosemide, citalopram, diclofenac, atorvastatin, and lorazepam occurs through the dehalogenation of the halogens, *i.e.* chlorine, and fluorine atoms based on the chemical structure (Appendix A **Fig. S2D, E, F, G, and H**). Degradation of chlorinated compounds by bio-Pd NPs has been thoroughly studied and it was shown that the halogens were often released first (Quan et al., 2018). Therefore, it is assumed that dechlorination occurred for furosemide, diclofenac, and lorazepam, which resulted in removal efficiencies of 89.7% ± 2.0%, 91.9% ± 2.8%, and 97.2% ± 0.7%, respectively. However, De Gusseme et al. (2012) found complete removal of diclofenac, through dechlorination. The difference in removal is due to the complex composition of the WWTP effluent tested in this work, where a complex mixture of micropollutants was present. The Pd-H bonds on the bio-Pd NPs used for the removal of compounds were not only occupied by diclofenac but also by other micropollutants present in the wastewater, therefore, lower removal of diclofenac can be expected. The advantage of using bio-Pd NPs is that only a single by-product is formed, which decreases the production of undesired, toxic, and mutagenic intermediates (De Gusseme et al., 2012). Removal of fluorinated micropollutants was also presumed for citalopram and atorvastatin, with removal efficiencies of 91.7% ± 0.4% and > 94.3%. Removal of ciprofloxacin through the use of bio-Pd NPs was established by He et al. (2020). It was suggested that defluorination, was one of the possible degradation processes that occurred as a first step (He et al., 2020). Defluorination of micropollutants is often obtained through AOP or adsorption (Alamgholiloo et al., 2021; Long et al., 2021). The AOP has been extensively investigated, and therefore different types of AOP exist, however, the

Table 1 – Concentration and removal efficiencies of emerging compounds in treated municipal secondary wastewater (real ww), with t_0 the concentration at the start of the experiment = 0 min, t_1 the concentration of the emerging compounds at 2 hr, and t_2 the concentration of the emerging compounds after 24 hr of bio-Pd NPs treatment.

Compounds	t_0 (ng/L)	t_1: real ww treated for 2 hr (ng/L)	t_2: real ww treated for 24 hr (ng/L)	t_1: Removal efficiency of treated ww (%)	t_2: Removal efficiency of treated ww (%)
Atorvastatin	57.7	5.6	< 1.0	> 94.3	> 98.3
Citalopram	119.5	9.9 ± 0.4	< 11.8	91.7 ± 0.4	> 95.0
Diclofenac	895.0	72.1 ± 25.0	59.7 ± 31.8	91.9 ± 2.8	93.3 ± 3.6
Furosemide	1233.6	126.9 ± 24.2	96.2 ± 50.7	89.7 ± 2.0	92.2 ± 4.1
Ibuprofen	2004.5	611.7 ± 27.9	752.8 ± 347.5	69.5 ± 1.4	62.4 ± 17.3
Lorazepam	285.0	8.1 ± 1.9	5.3 ± 5.4	97.2 ± 0.7	98.1 ± 1.9
Naproxen	6893.6	1279.9 ± 463.1	929.5 ± 254.4	81.4 ± 6.7	86.5 ± 3.7
Sulfamethoxazole	521.7	101.1 ± 30.7	86.9 ± 4.5	80.6 ± 5.9	83.3 ± 0.9

disadvantage of this method is that requirements need to be met before using this method. As such, catalysts are desired due to maximizing the removal potential, presence of light, and addition of iron (Chin et al., 2014; Olvera-Vargas et al., 2015; Bartolomeu et al., 2018). The use of bio-Pd NPs has more advantages demonstrated by the high removal efficiency of halogenated compounds. After dehalogenation, it is proposed that further degradation of the C=O bond, C-C bond and aromatic structures will occur through hydrogenation by bio-Pd NPs (Kluson and Cerveny, 1995; Adams et al., 2014).

Besides dehalogenation, the removal of ibuprofen, sulfamethoxazole, and naproxen was also found. The controls proved that removal was obtained from the catalytic activity of bio-Pd NPs rather than from adsorption or biodegradation. It is suggested that the removal of these three compounds by bio-Pd NPs was obtained through carbon-carbon and carbon-heteroatom cross-coupling reaction (Adams et al., 2014). It is presumed that aromatic compounds will be hydrogenated afterwards (Zhang et al., 2022). Although ibuprofen and sulfamethoxazole removal were low in this study compared to the other compounds, 69.5% ± 1.4%, and 80.6% ± 5.9%, respectively, the degradation was still relatively high and fast compared to what was reported by Martins et al. (2017) and Forrez et al. (2011). Martins et al. (2017) found no removal of ibuprofen and 85% degradation of sulfamethoxazole after 24 hr of treatment with bio-Pd and bio-Pt NPs. Removal was not observed for ibuprofen partially due to the absence of adsorption (Martins et al., 2017). The degradation of ibuprofen and sulfamethoxazole with biogenic metals manganese oxide was obtained after 13 days, with concentrations decreasing from 158 to < 8 ng/L and from 259 to 256 ng/L, respectively (Forrez et al., 2011). Removal efficiencies of 81.4% ± 6.7% were obtained for naproxen in this work, which is high compared to biodegradation with *Trametes versicolor* for which 31% degradation was obtained after 24 hr (Bernats and Juhna, 2018). Biogenic metals manganese oxide was also tested by Forrez et al. (2011), but no removal was observed for naproxen after 13 days.

3. Conclusion

Steering the production of bio-Pd NPs is possible through the use of an EC for the supply of H_2 as an electron donor. In contrast to a previous hypothesis and earlier works, a lower flow rate of H_2 resulted in larger bio-Pd NPs (39.0 nm) showing higher catalytic activity, compared to the smaller NPs (23.2 nm). However, the lowest catalytic activity of the nanoparticles was found for the largest nanoparticles (> 100 nm). It was observed that the size of the NPs is independent of the conversion efficiency of Pd^{2+}, as the most catalytic active bio-Pd NPs showed the lowest conversion efficiency, with a NPs size of 39.0 nm. High removal efficiencies of these bio-Pd NPs were also found for the reductive transformation of persistent micropollutants that was present in complex matrices with environmentally relevant concentrations in 2 hr. An effect of the bio-Pd NPs on the dehalogenation of fluorinated and chlorinated pharmaceutical compounds was also proposed in this study. Another advantage of the use of bio-Pd NPs is the low mass of palladium that was used. Although palladium is expensive, high removal efficiencies are obtained in a shorter time. This study provides strong support for the use of bio-Pd NPs to efficiently remove micropollutants from the environment and the possible applicability to WWTP as a tertiary treatment system. However, before applying bio-Pd NPs in real wastewater treatment systems, more investigation is required. H_2 can be submitted by implementing an electrochemical system into the treatment plant or more research can be performed on finding an alternative electron donor for the reductive dehalogenation of halogenated micropollutants by the catalytic activity of the bio-Pd NPs. Besides this, it is also important to recover bio-Pd NPs for economical feasibility. Recovery of Pd^{2+} from the supernatant solution, after production of bio-Pd NPs, can be achieved by the addition of *Shewanella oneidensis* to the solution, as the matrices of the cells and the supernatants are the same. It is also possible to recover leaching Pd NPs from the bio-Pd NPs, by chemical reaction, hence by the addition of nitric acid, which has been performed by other researchers. Nevertheless, more research needs to be performed on the application of bio-Pd NPs as the recovery of Pd.

Declaration of Competing Interest

The authors declare that they have no known competing financial interests or personal relationships that could have appeared to influence the work reported in this article.

Acknowledgments

The ELECTRA project has received funding from European Union's Horizon 2020 research and innovation program under grant agreement No. 826244. Eduardo Bolea-Fernandez thanks FWO-Vlaanderen for his postdoctoral grant (No. 12ZA320N). The authors would like to thank Victor Lobanov, Mingsheng Jia, and Hira Khan for critically reading the manuscript.

Appendix A Supplementary data

Supplementary material associated with this article can be found, in the online version, at doi:10.1016/j.jes.2022.08.018.

REFERENCE

Abtahi, S.M., Ilyas, S., Joannis Cassan, C., Albasi, C., de Vos, W.M., 2018. Micropollutants removal from secondary-treated municipal wastewater using weak polyelectrolyte multilayer based nanofiltration membranes. J. Membr. Sci. 548, 654–666.

Adams, C.P., Walker, K.A., Obare, S.O., Docherty, K.M., 2014. Size-dependent antimicrobial effects of novel palladium nanoparticles. PLoS One 9, e85981.

Alamgholiloo, H., Pesyan, N.N., Mohammadi, R., Rostamnia, S., Shokouhimehr, M., 2021. Synergistic advanced oxidation process for the fast degradation of ciprofloxacin antibiotics using a GO/CuMOF-magnetic ternary nanocomposite. J. Environ. Chem. Eng. 9, 105486.

Anjali, R., Shanthakumar, S., 2019. Insights on the current status of occurrence and removal of antibiotics in wastewater by advanced oxidation processes. J. Environ. Manage 246, 51–62.

Antonelli, R., Malpass, G.R.P., da Silva, M.G.C., Vieira, M.G.A., 2020. Adsorption of ciprofloxacin onto thermally modified bentonite clay: Experimental design, characterization, and adsorbent regeneration. J. Environ. Chem. Eng. 8, 104553.

Bartolomeu, M., Neves, M.G.P.M.S., Faustino, M.A.F., Almeida, A., 2018. Wastewater chemical contaminants: remediation by advanced oxidation processes. Photochem. Photobiol. Sci. 17, 1573–1598.

Bernats, M., Juhna, T., 2018. Removal of phenols-like substances in pharmaceutical wastewater with fungal bioreactors by adding Trametes versicolor. Water Sci. Technol. 78, 743–750.

Bobu, M., Yediler, A., Siminiceanu, I., Zhang, F., Schulte-Hostede, S., 2013. Comparison of different advanced oxidation processes for the degradation of two fluoroquinolone antibiotics in aqueous solutions. J. Environ. Sci. Health. Toxic/hazardous Substance Environ. Eng. 48, 251–262.

Cao, Z., Liu, X., Xu, J., Zhang, J., Yang, Y., Zhou, J., et al., 2017. Removal of antibiotic Florfenicol by sulfide-modified nanoscale zero-valent iron. ES&T 51, 11269–11277.

Chen, Y., Chen, Y, 2021. Difference in toxicity of Pd (II) and mechanism of action before and after reduction by Bacillus wiedmannii MSM. Environ. Sci. Pollut. Res. 29, 1824–1835.

Chin, C.J.M., Chen, T.Y., Lee, M., Chang, C.F., Liu, Y.T., Kuo, Y.T., 2014. Effective anodic oxidation of naproxen by platinum nanoparticles coated FTO glass. J. Hazard. Mater. 277, 110–119.

de Andrade, J.R., Oliveira, M.F., da Silva, M.G.C., Vieira, M.G.A., 2018. Adsorption of pharmaceuticals from water and wastewater using nonconventional low-cost materials: a review. Ind. Eng. Chem. Res. 57, 3103–3127.

De Corte, S., Sabbe, T., Hennebel, T., Vanhaecke, L., De Gusseme, B., Verstraete, W., Boon, N., 2012. Doping of biogenic Pd catalysts with Au enables dechlorination of diclofenac at environmental conditions. Water Res. 46, 2718–2726.

De Gusseme, B., Soetaert, M., Hennebel, T., Vanhaecke, L., Boon, N., Verstraete, W., 2012. Catalytic dechlorination of diclofenac by biogenic palladium in a microbial electrolysis cell. Microb. Biotechnol. 5, 396–402.

de Santiago-Martín, A., Meffe, R., Teijón, G., Martínez Hernández, V., López-Heras, I., Alonso Alonso, C., et al., 2020. Pharmaceuticals and trace metals in the surface water used for crop irrigation: risk to health or natural attenuation? Sci. Total Environ. 705, 135825.

De Windt, W., Aelterman, P., Verstraete, W., et al., 2005. Bioreductive deposition of palladium (0) nanoparticles on Shewanella oneidensis with catalytic activity towards reductive dechlorination of polychlorinated biphenyls. Appl. Micro. Int. 7 (3), 314–325.

De Windt, W., Boon, N., Van den Bulcke, J., Rubberecht, L., Prata, F., Mast, J., et al., 2006. Biological control of the size and reactivity of catalytic Pd(0) produced by Shewanella oneidensis. Antonie Van Leeuwenhoek 90, 377–389.

Deplanche, K., Bennett, J.A., Mikheenko, I.P., Omajali, J., Wells, A.S., Meadows, R.E., et al., 2014. Catalytic activity of biomass-supported Pd nanoparticles: Influence of the biological component in catalytic efficacy and potential application in 'green' synthesis of fine chemicals and pharmaceuticals. Appl. Catal. 147, 651–665.

Dundas, C.M., Graham, A.J., Romanovicz, D.K., Keitz, B.K., 2018. Extracellular electron transfer by shewanella oneidensis controls palladium nanoparticle phenotype. ACS Synth. Biol. 7, 2726–2736.

Ershov, B.G., Solovov, R.D., Abkhalimov, E.V., 2014. Palladium nanoparticles in aqueous solution: Preparation, properties, and effect of their size on catalytic activity. Colloid J. 76, 553–557.

Forrez, I., Carballa, M., Fink, G., Wick, A., Hennebel, T., Vanhaecke, L., et al., 2011. Biogenic metals for the oxidative and reductive removal of pharmaceuticals, biocides and iodinated contrast media in a polishing membrane bioreactor. Water Res. 45, 1763–1773.

Freitas, N.S., Alzamora, M., Sánchez, D.R., Licea, Y.E., Senra, J.D., Carvalho, N.M.F., 2021. Green palladium nanoparticles prepared with glycerol and supported on maghemite for dye removal application. J. Environ. Chem. Eng. 9, 104856.

Gautam, P.K., Singh, A., Misra, K., Sahoo, A.K., Samanta, S.K., 2019. Synthesis and applications of biogenic nanomaterials in drinking and wastewater treatment. Environ. Manage. 231, 734–748.

Gomez-Bolivar, J., Mikheenko, I.P., Orozco, R.L., Sharma, S., Banerjee, D., Walker, M., et al., 2019. Synthesis of Pd/Ru bimetallic nanoparticles by escherichia coli and potential as a catalyst for upgrading 5-Hydroxymethyl furfural into liquid fuel precursors. Front. Microbiol. 1276.

Han, J., Hu, W., Deng, H., 2009. Adsorption of hydrogen on palladium nanoparticle surfaces. Surf. Interface Anal. 41, 590–594.

Hazarika, M., Borah, D., Bora, P., Silva, A.R., Das, P., 2017. Biogenic synthesis of palladium nanoparticles and their applications as catalyst and antimicrobial agent. PLoS One 12, e0184936.

He, P., Mao, T., Wang, A., Yin, Y., Shen, J., Chen, H., Zhang, P., 2020. Enhanced reductive removal of ciprofloxacin in pharmaceutical wastewater using biogenic palladium nanoparticles by bubbling H2. RSC Adv. 10, 26067–26077.

Hennebel, T., Benner, J., Clauwaert, P., Vanhaecke, L., Aelterman, P., Callebaut, R., et al., 2011. Dehalogenation of environmental pollutants in microbial electrolysis cells with biogenic palladium nanoparticles. Biotechnol. Lett. 33, 89–95 .

Hou, Y.N., Zhang, B., Yun, H., Yang, Z.N., Han, J.L., Zhou, J., et al., 2017. Palladized cells as suspension catalyst and

electrochemical catalyst for reductively degrading aromatics contaminants: Roles of Pd size and distribution. Water Res. 125, 288–297.
Jiang, W.L., Ding, Y.C., Haider, M.R., Han, J.L., Liang, B., Xia, X., et al., 2020. A novel TiO2/graphite felt photoanode assisted electro-Fenton catalytic membrane process for sequential degradation of antibiotic florfenicol and elimination of its antibacterial activity. Chem. Eng. J. 391, 123503.
Khataee, A.R., Kasiri, M.B., 2010. Photocatalytic degradation of organic dyes in the presence of nanostructured titanium dioxide: Influence of the chemical structure of dyes. J. Mol. Catal. A Chem. 328, 8–26.
Kluson, P., Cerveny, L., 1995. Selective hydrogenation over ruthenium catalysts. Appl. Catal. 128, 13–31.
Liu, H., Han, J., Yuan, J., Liu, C., Wang, D., Liu, T., et al., 2019. Deep dehalogenation of Florfenicol Using Crystalline CoP Nanosheet Arrays on a Ti Plate via direct cathodic reduction and atomic H. ES&T 53, 11932–11940.
Long, M., Donoso, J., Bhati, M., Elias, W.C., Heck, K.N., Luo, Y.H., et al., 2021. Adsorption and reductive defluorination of perfluorooctanoic acid over palladium nanoparticles. ES&T 55, 14836–14843.
Lovley, D.R., 1993. Dissimilatory metal reduction. Ann. Rev. Microbiol. 47, 263–290.
Martins, M., Mourato, C., Sanches, S., Noronha, J.P., Crespo, M.T.B., Pereira, I.A.C., 2017. Biogenic platinum and palladium nanoparticles as new catalysts for the removal of pharmaceutical compounds. Water Res. 108, 160–168.
Miao, D., Peng, J., Wang, M., Shao, S., Wang, L., Gao, S., 2018. Removal of atorvastatin in water mediated by CuFe2O4 activated peroxymonosulfate. Chem. Eng. J. 346, 1–10.
Nguyen, C.H., Fu, C.C., Juang, R.S., 2018. Degradation of methylene blue and methyl orange by palladium-doped TiO2 photocatalysis for water reuse: Efficiency and degradation pathways. J. Clean. Prod. 202, 413–427.
Olvera-Vargas, H., Oturan, N., Buisson, D., van Hullebusch, E.D., Oturan, M.A., 2015. Electro-oxidation of the pharmaceutical furosemide: kinetics, mechanism, and By-Products. clean. 43, 1455–1463 Weinh.
Omajali, J.B., Gomez-Bolivar, J., Mikheenko, I.P., Sharma, S., Kayode, B., Al-Duri, B., et al., 2019. Novel catalytically active Pd/Ru bimetallic nanoparticles synthesized by Bacillus benzeovorans. Sci. Rep. 9, 4715.
Osawa, R.A., Carvalho, A.P., Monteiro, O.C., Oliveira, M.C., Florêncio, M.H., 2019. Transformation products of citalopram: Identification, wastewater analysis and in silico toxicological assessment. Chemosphere 217, 858–868.
Pandey, A., Shukla, P., Srivastava, P., 2020. Remediation of dyes in water using green synthesized nanoparticles (NPs). IJPE 6, 68–84.
Peñacoba-Antona, L., Senán-Salinas, J., Aguirre-Sierra, A., Letón, P., Salas, J.J., García-Calvo, E., et al., 2021. Assessing METland® design and performance through LCA: techno-environmental study with multifunctional unit perspective. Front. Microbiol. 12, 652173.
Quan, X., Zhang, X., Sun, Y., Zhao, J., 2018. Iohexol degradation by biogenic palladium nanoparticles hosted in anaerobic granular sludge. Front. Microbiol. 9, 1980.
Rotaru, A.-E., Jiang, W., Finster, K., Skrydstrup, T., Meyer, R.L., 2012. Non-enzymatic palladium recovery on microbial and synthetic surfaces. Biotechnol. Bioeng. 109, 1889–1897.
Saldan, I., Semenyuk, Y., Marchuk, I., Reshetnyak, O., 2015. Chemical synthesis and application of palladium nanoparticles. J. Mater. Sci. 50, 2337–2354.
Sivamaruthi, B.S., Ramkumar, V.S., Archunan, G., Chaiyasut, C., Suganthy, N., 2019. Biogenic synthesis of silver palladium bimetallic nanoparticles from fruit extract of Terminalia chebula – In vitro evaluation of anticancer and antimicrobial activity. J Drug Deliv Sci Technol 51, 139–151.
Tuo, Y., Liu, G., Dong, B., Yu, H., Zhou, J., Wang, J., Jin, R, 2017. Microbial synthesis of bimetallic PdPt nanoparticles for catalytic reduction of 4-nitrophenol. Environ. Sci. Pollut. Res. 24, 5249–5258.
Wang, P.T., Song, Y.H., Fan, H.C., Yu, L., 2018. Bioreduction of azo dyes was enhanced by in-situ biogenic palladium nanoparticles. Bioresour. Technol. 266, 176–180.
Xiong, L., Zhang, X., Huang, Y.X., Liu, W.J., Chen, Y.L., Yu, S.S., et al., 2018. Biogenic synthesis of Pd-Based nanoparticles with enhanced catalytic activity. ACS Appl. Nano Mater. 1, 1467–1475.
Xu, H., Tan, L., Cui, H., Xu, M., Xiao, Y., Wu, H., et al., 2018. Characterization of Pd(II) biosorption in aqueous solution by Shewanella oneidensis MR-1. J. Mol. Liq. 255, 333–340.
Yagub, M.T., Sen, T.K., Afroze, S., Ang, H.M., 2014. Dye and its removal from aqueous solution by adsorption: a review. Adv. Colloid Interface Sci. 209, 172–184.
Yang, Z.-N., Hou, Y.-N., Zhang, B., Cheng, H.-Y., Yong, Y.-C., Liu, W.-Z., et al., 2020. Insights into palladium nanoparticles produced by Shewanella oneidensis MR-1: Roles of NADH dehydrogenases and hydrogenases. Environ. Res. 191, 110196.
Yudanov, I.V., Genest, A., Rösch, N., 2011. DFT studies of palladium model catalysts: structure and size effects. J. Clust. Sci 22, 433–448.
Yudanov, I.V., Sahnoun, R., Neyman, K.M., Rösch, N., Hoffmann, J., Schauermann, S., et al., 2003. CO adsorption on pd nanoparticles: density functional and vibrational spectroscopy studies. J. Phys. Chem. B 107, 255–264.
Zhang, M., Song, Q., He, Z., Wang, Q., Wang, L., Zhang, X., Li, G., 2022. Tuning the mesopore-acid-metal balance in Pd/HY for efficient deep hydrogenation saturation of naphthalene. Int. J. Hydrog. Energy 47, 20881–20893.